PAPER • **OPEN ACCESS**

From the ReRu-rich δ Phase to the Intergrowth of the P and the σ Phases in Ru-bearing Ni-base Superalloys

To cite this article: Chunhui Wang *et al* 2019 *IOP Conf. Ser.: Mater. Sci. Eng.* **562** 012021

IOP Conf. Series: Materials Science and Engineering **562** (2019) 012021 doi:10.1088/1757-899X/562/1/012021

From the ReRu-rich δ Phase to the Intergrowth of the P and the σ Phases in Ru-bearing Ni-base Superalloys

Chunhui Wang, Yanhui Chen[1*], Jingyang Chen[2], Fei Xue[2], Wei Li[1] and Luyan Yang[1]

[1]Institute of the Microstructure and Properties of Advanced Materials, Beijing University of Technology, 100124, Beijing, china,
[2]Science and Technology of Advanced High-Temperature Structural Materials Laboratory, Beijing Institute of Aeronautical Materials, 100095, Beijing, china
Corresponding Author: yhchen@bjut.edu.cn

Abstract. The morphology, composition, structure and formation mechanisms of precipitates in three Ni-base single crystal superalloys containing 3.2 at. % Ru by adding Cr (0 to 6.5 at. %) were investigated. The precipitation speed in the Low-Cr alloy was low at a temperature of 1100 °C. The ReRu-rich δ phase, with a hexagonal structure, was the primary phase. A high quantity of precipitates appeared in the high Cr alloy after 50 h of heat treatment. The quantity increased rapidly from that time. The σ phases dominated the precipitate after a short period of heating at 1100 °C, with the orientation relationship corresponding to $[111]_{\gamma/\gamma'}$// $[111]_{\sigma}$ and $(110)_{\gamma/\gamma'}$ // $(110)_{\sigma}$. The σ phase transformed into the intergrowth of the σ and the P phases discontinuously through the σ needle as the exposure time increased. The large elemental γ/γ′ partitioning ratio of Re in 6.5 at. % Cr was the key factor that promoted nucleation in the σ phase.

1. Introduction

The major advancement in third-generation alloys was achieved through the addition of rhenium (Re), which enabled a significant increase in the creep capability over earlier generation alloys[1][2]. However, if the concentration of Re and other refractory elements are greater than their solubility, topologically close-packed (TCP) phases may form during long-term thermal exposure, which will seriously deteriorate creep strength[3]. Based on third-generation superalloys, ruthenium (Ru)-bearing Ni-based superalloys have been heavily researched because they have a stable microstructure. The addition of Ru prohibits the precipitation of TCP during high-temperature service of the alloys by decreasing the element partitioning of Re in the γ phase[4][5]. Ru is a refractory element, and its addition to superalloys can effectively strengthen the γ and γ′ phases[6][7][8].

Chromium (Cr) is generally added to Ni-based superalloys because it is aids in hot corrosion resistance and oxidation resistance. In addition, Cr is an effective solid-solution strengthener[9]. Modern commercial Ni-based single crystals[10] and directionally solidified[11] superalloys contain moderate amounts of Cr. However, at high levels of Cr, detrimental TCP phases occur[12]. To optimize the physical and mechanical properties of Ni-based superalloys, a detailed understanding of the effect of Cr on the microstructure and on the precipitation process of Ru-bearing Ni-based superalloys is necessary. In our early work[13], we reported on the microstructural variation in the γ/γ' matrix and precipitates in alloys that contained high levels of Cr and Ru. An understanding of the detailed crystallographic structures and their formation mechanism is still required.

Furthermore, it has been reported that Ru-containing Ni-based alloys precipitate a hexagonally structured δ phase[14], which is different than the precipitate from conventional TCP phases. The precipitation of the δ phase in a series of Ru-bearing single crystal superalloys was first reported in 2003[15]. Because this study is focusing on Ru-bearing single crystal superalloys, the precipitation of the δ phase is therefore expected to appear based on that previous study. It is therefore important to detail the precipitation process and its formation factors. Furthermore, this process must be compared with the conventional TCP phase process to aid in the development of this new generation of superalloys.

The objective of this study is to investigate the morphological and structural variations in the precipitates of high levels of Ru-bearing (3.2 at. %) Ni-based single crystal alloys during thermal exposure with the addition of different levels of Cr (0-6.5 at.%). The primary factors that affect the formation of the δ phase and of the TCP phases will also be discussed. The intergrowth of the two TCP phases in High-Cr alloys will also be presented.

2. Experimental Procedure

Three experimental fourth-generation alloys containing 1.6 at. % Re and 3.2 at. % Ru were considered. The compositions, shown in table 1, vary systemically in Cr concentration, at 0 at. %, 3.5 at. % and 6.5 at.%. The materials were all vacuum induction melted (VIM), and selected alloys from among this set were directionally solidified (DS) into cylindrical bars in ceramic cluster molds in a Bridgman furnace at a withdrawal rate of 200 mm/h.

Table 1. Nominal compositions of the investigated alloys (at.%).

Alloy	Ni	Al	Ta	W	Co	Re	Cr	Ru
USTB-0Cr	Bal.	13.7	2.8	1.9	7.8	1.6	0	3.2
USTB-3.5Cr	Bal.	14.3	2.7	2.0	7.6	1.6	3.5	3.2
USTB-6.5Cr	Bal.	14.5	2.8	2.0	7.7	1.6	6.5	3.2

Conventional helical starters were used to initiate single crystal growth. Heat treatment experiments were conducted on oversized samples in a tube furnace in an air atmosphere. In this study, the investigated alloys were heated in a two-step procedure: (1) a solution treatment, consisting of thermal exposure at 1300 °C for 4 h with a subsequent water quench followed by (2) a thermal exposure treatment, consisting of thermal exposure at 1100 °C for 50 h, 800 h, 1000 h, 1500 h and 2000 h. As-cast and heat-treated specimens for microstructural examination were prepared by standard metallographic procedures and etched in an etchant of 1% HF, 33% CH_3COOH, 33% HNO_3 and 33% H_2O. The specimens were studied with a ZEISS SUPRA 55FEG scanning electron microscope (SEM) operated in the secondary electron (SE) imaging modes. The specimens for transmission electron microscopy were prepared by twin-jet electro-polishing techniques in a solution of 10% perchloric acid, 9% distilled water, 13% butyl cellusolve and 68% methanol at -40 °C and 20 V. A JEOL 2010 electron microscope was used to identify and analyse the phases using selected area electron diffraction (SAED), and energy dispersive spectroscopy (EDX). Samples were sectioned on {111} to increase the probability that the TCP phases will be near a low index orientation, which would thus facilitate the identification of the phases. Selected area diffraction (SAD) patterns were obtained via transmission electron microscopy (TEM).

3. Results

As reported in our previous works[16][17][18], no additional phases beyond the γ or γ′ phases were observed in the as-solidified or solution-treated microstructures.

3.1. Alloy USTB-0Cr

After aging at 1100 °C for 1000 h, short needle-like precipitates on the order of a few micrometres long are visible among the γ/γ′ matrix in alloy USTB-0Cr, as shown in the SEM image in Figure 1a, where the viewing direction is parallel to the <001> growth direction. A typical SEM image of

precipitates embedded within the γ/γ′ matrix in the alloy aged for 2000 h is shown in Figure 1b. The data in this figure show no morphological variation. A statistical analysis indicated that the quantity of precipitates did not change substantively between the alloy aged for 1000 h and that aged for 2000 h. The data in the bright field TEM image in Figure 1c show one sheet of plate-like precipitation that lies on the matrix. The electron diffraction pattern (EDP) along the [221] direction of this precipitation, shown in Figure 1d, indicates it is of the hexagonal Re/Ru type (P63/mmc, a=2.7 Å, c=4.4 Å, α=90^o, γ=120^o). The chemical composition of the precipitate measured by EDX in the TEM is shown in table 2. The data in the table show that, except for the base element Ni and small amounts of Al and Co, Re and Ru were the primary elements at a ratio of 1:1, which is similar to the hexagonal δ-Re0.54Ru0.46 phase (P63/mmc, a=2.7 Å, c=4.3 Å, α=90^o, γ=120^o).

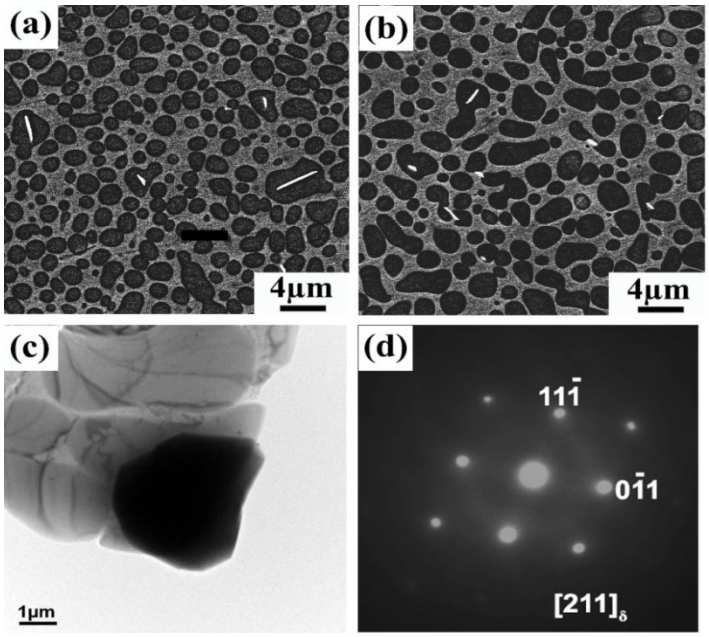

Figure 1. Typical SE images of alloy USTB-0Cr after aging at 1100 °C for (a) 1000 h and (b) 2000 h, (c) Bright field TEM image of a region containing plate-like precipitates in USTB-0Cr alloys aged at 1100 °C for 1000 h, (d) the SAED pattern in c.

Table 2. Average chemical composition (at. %) of the precipitation in alloy 0Cr after thermal exposure at 1100°C for 1000 h.

Element	Precipitation(at.%)
Ni	51.8
Al	7.8
Co	8.6
Re	17.1
Ru	14.7

3.2. Alloy USTB-3.5Cr

Figures 2a-b show representative SEM images of USTB-3.5Cr alloy after exposure at 1100 ºC for 1000 h and 2000 h, respectively. Needle- and disc-like precipitates formed in the USTB-3.5Cr alloy with a similar morphology and volume fraction as those observed in the USTB-0Cr alloy. An increase in the γ′ phase was observed in the USTB-3.5Cr alloy. The results indicate that adding Cr alters the morphology from spherical to cubic and reduces the thermal stability of the superalloy. Figures 2c-d show the bright field TEM image and the corresponding SAED pattern of the precipitate. The data in those figures show that the precipitate has the same crystallographic structure as that formed in the USTB-0Cr alloy. The energy dispersive x-ray spectroscopy (EDS) analysis indicates that the

precipitation was rich in Re and Ru with an average Re/Ru ratio of approximately 2, as shown in table 3 (37 at. % Re and 20.7 at. % Ru). The precipitates, in total, contained 57.7 at. % Re and Ru elements, which is much greater than the composition of the USTB-3.5Cr alloy itself (31.8 at.%). It is known that $Re_{0.9}Ru_{0.1}$, $Re_{0.54}Ru_{0.46}$ and Re have the same crystallographic structure of P63/mmc, where a=2.7 Å, c=4.3 Å, $\alpha=90^{o}$ and $\gamma=120^{o}$. The precipitates of the alloy USTB-3.5Cr can be seen as a solid solution of Re and Ru with a hexagonal Re structure (also the same as $Re_{0.9}Ru_{0.1}$ and $Re_{0.54}Ru_{0.46}$).

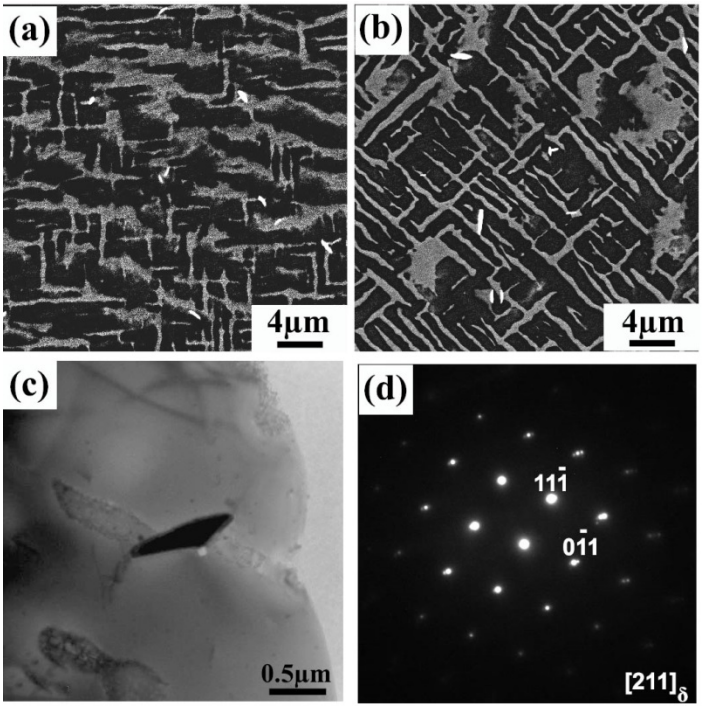

Figure 2. Representative microstructures of the USTB-3.5Cr alloy after exposure at 1100 ºC for (a) 1000 h and (b) 2000 h. (c) Bright field TEM image of the USTB-3.5Cr alloy after exposure at 1100 ºC for 1000 h. (d) The corresponding SAED pattern of the precipitate.

Table 3. Chemical composition (at. %) of the precipitation from sample 3.5Cr after thermal exposure at 1100 °C for 1000 h.

Element	Precipitation(at.%)
Ni	28.1
Co	8.7
Re	5.3
Re	37.0
Ru	20.9

3.3. Alloy USTB-6.5Cr

Figures 3a-b show the SEM image of the 6.5 at. % Cr alloy after thermal exposure at 1100 ºC for 50 h and 800 h, respectively. Needle-like precipitates with lengths of tens of micrometres and morphologies similar to the TCP phases formed in the specimen after a short exposure time of 50 h. A large fraction of precipitates with a much larger length of over 100 μm formed during prolonged exposure at 800 h (Figure 3b). The results indicated that the addition of 6.5 at. % Cr accelerates the nucleation and growth rate of the precipitate and improves the regularity of the γ′ phase.

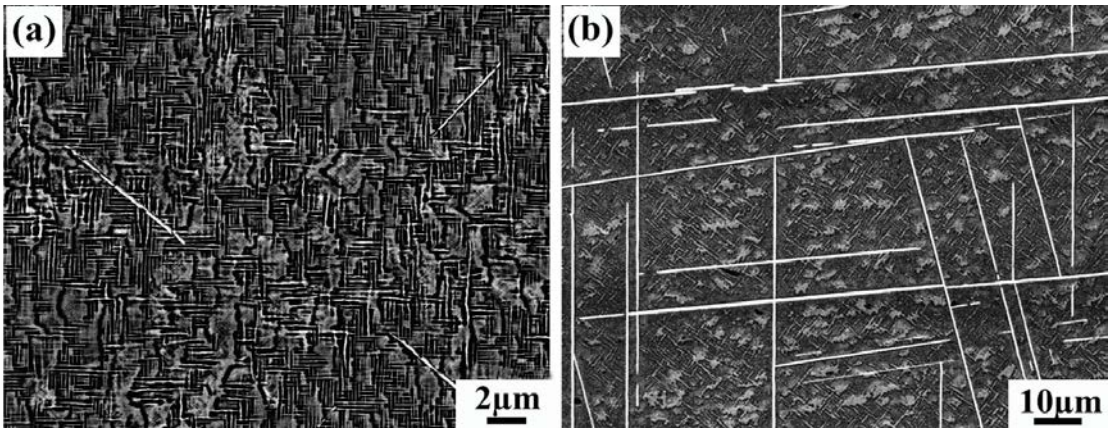

Figure 3. (a) SEM micrograph of alloy USTB-6.5Cr after thermal exposure at 1100 °C for 50 h and (b) 800 h

Figures 4a-b show the bright field TEM image and the corresponding SAED pattern of the precipitate formed in the 6.5 at. % Cr alloy after exposure at 1100 ºC for 50 h. The SAED pattern contains two sets of diffraction patterns; the bright set corresponds to the γ/γ′ matrix and the faint set is indexed as the σ phase (P42/mnm, a=9.1 Å, c=4.7 Å, α=90°). The orientation relationship between the two sets of patterns were determined to be $[111]_{\gamma/\gamma'}$// $[111]_{\sigma}$ and $(110)_{\gamma\gamma'}$// $(110)_{\sigma}$. Figure 4c is a typical high-resolution transmission electron microscope (HRTEM) image at a distance of 0.9 nm between two adjacent clusters, indexed by circles. Experimental data on other precipitates were also identified as the σ phase.

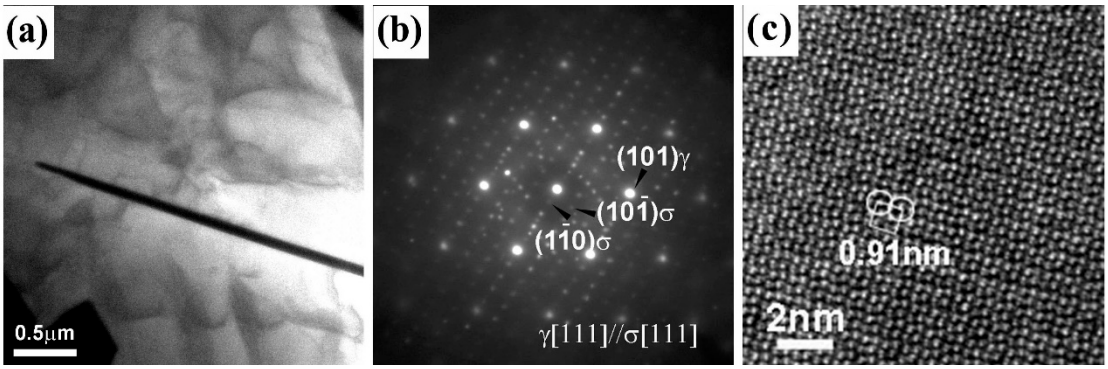

Figure 4. (a) Bright field TEM image of precipitates in alloy USTB-6.5Cr after thermal exposure at 1100°C for 50 h and (b) Corresponding EDP of (a). (c) HRTEM image between two adjacent clusters

Figure 5a is a TEM image of the precipitate formed in USTB-6.5Cr after exposure at 1100 ºC for 800 h. Four regions, marked as A-D in Figure 5a, were subjected to SAED analysis. The SAED patterns of regions A and C in Figure 5b can be attributed to the same crystal of the σ phase. The SAED patterns of regions B and D have the same pattern as that shown in Figure 5c and are indexed as the P phase (Pnma, a=9.0 Å, b=16.9 Å, c=4.7 Å, α=90°). The results indicated that a transformation from the σ phase to the P phase occurred during the prolonged exposure time in a random mode instead of a continuous mode.

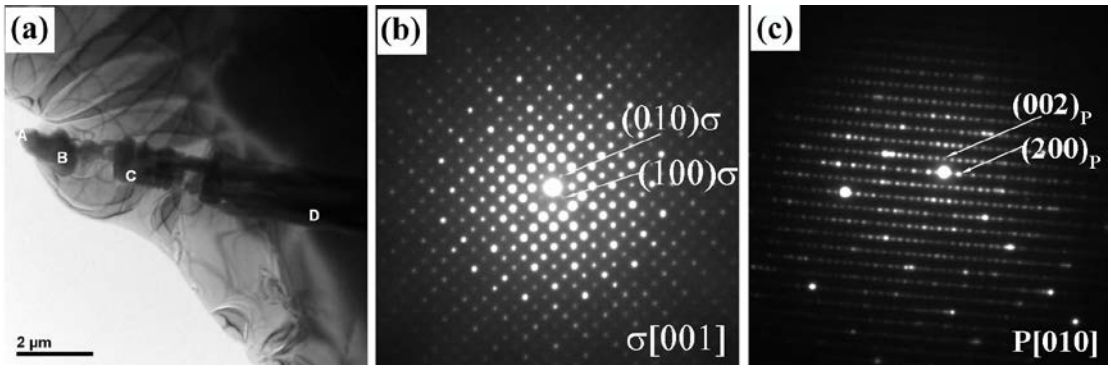

Figure 5. TEM identification of the precipitate in the USTB-6.5Cr alloy after thermal exposure at 1100 ºC for 800 h.
(a) Bright field TEM image. (b) SAED pattern of region A. (c) SAED pattern of region B.

The chemical compositions of the two types of precipitates were measured using EDS in TEM. The results are listed in table 4. All of the precipitates are rich in Cr and Re in a ratio of approximately 2:3. The fraction of Cr and Re is higher in the precipitate formed after exposure for 800 h than that formed after exposure for 50 h, which indicates a gradual concentration of these elements in the precipitates with prolonged exposure time. The fraction of Re is higher in the P phase than in the σ phase.

Table 4. Chemical compositions (at. %) of precipitates from the 6.5 at. % Cr alloy after thermal exposure at 1100 ºC.

Element	50 h(σ)	800 h(σ)	800 h(P)
Al	0.89	-	-
Cr	17.4	20.19	12.98
Co	8.86	8.94	6.64
Ni	35.15	12.99	15.99
Ru	2.83	7.70	8.52
Ta	3.00	7.71	13.92
W	10.82	13.66	9.74
Re	21.05	28.81	32.21

4. Discussion

Table 5 summarizes the type and quantity of precipitates formed in the three specimens after thermal exposure at 1100 ºC for different times. The addition of 3.5 at. % Cr only slightly influences the precipitation, even after a long exposure time of 2000 h; however, it changes the morphology of the γ′ phase. The addition of 6.5 at. % Cr has influences the precipitate in two ways. First, it remarkably reduces the incubation time, from ~1000 h to less than 50 h, resulting in an increase in the quantity of precipitates and the growth rate of the precipitate. Second, it produces a variation in the type of precipitate, from the δ phase in the USTB-0Cr and USTB-3.5Cr alloys, to the σ and P phases in the USTB-6.5Cr alloy. Style and Spacing.

Table 5. Precipitate type and quantity obtained in the three specimens after different exposure times.

Alloy	Detectable time (h)	Phase	Exposure time (h)	Phase
USTB-0Cr	1000	δ	2000	δ
USTB-3.5Cr	1000	δ	2000	δ
USTB-6.5Cr	50	σ	2000	σ + P

A typical component of the σ phase in Re superalloys, a precursor of TCPs, is Cr_2Re_3[18]. Therefore, the formation of the σ phase is inhibited in the USTB-0Cr alloy because of the absence of Cr. Precipitation of the δ-ReRu in the USTB-0Cr alloy is expected because the alloy contains a large amount of Re and Ru. It is well known that adding Cr promotes the supersaturated solid solubility of refractory elements, particularly the Re element, which is prone to form the TCP phases[19]. Table 6 lists the elemental γ/γ′ partitioning ratio (k_i) measured from the dendritic regions in the three alloys after exposure at 1100 ºC for 800 h. The k_i is defined as

$$k_i = \frac{C_i^{\gamma}}{C_i^{\gamma'}} \quad (1)$$

where C_i^{γ} and $C_i^{\gamma'}$ are the atomic concentrations of the element in the γ and γ′ phases, respectively. The k_i increases from 3.8 in the USTB-0Cr alloy to 7.6 in the USTB-3.5Cr alloy and to 20.2 in the USTB-6.5Cr alloy. It is thus reasonable to deduce that the large amount of aggregation of Re in the USTB-6.5Cr alloy from partitioning can promote the precipitation of the TCP phases[20].

Table 6. Elemental γ/γ′ partitioning ratios in the three alloys after thermal exposure at 1100 ºC for 800 h.

Alloy	Al	Cr	Co	Ni	Ru	Ta	W	Re
USTB-0Cr	0.61	-	1.47	-	1.28	0.56	1.43	3.80
USTB-3.5Cr	0.60	3.0	1.70	-	1.57	0.39	1.26	7.62
USTB-6.5Cr	0.54	2.97	1.71	-	1.98	0.14	1.28	20.20

5. Conclusion

The effect of Cr on the precipitation behaviours in three Ru-containing single-crystal Ni-based superalloys subjected to thermal exposure at 1100 ºC was studied. The conclusions are summarized as follows:

1. The addition of 3.5 at. % Cr slightly influences the precipitation behaviours. The precipitate in both of the alloys, i.e., free of Cr and 3.5 at. % Cr, was identified to be hexagonal-type δ phase, which is stable up to 2000 h of exposure.
2. The addition of 6.5 at. % Cr remarkably reduces the incubation time of the precipitate from ~1000 h in the Cr-free and 3.5 at. % Cr alloys to 50 h. The precipitate in the 6.5 at. % Cr alloy is the σ phase, which is a type of TCP phase. The σ phase transformed to the P phase discontinuously through the σ needles as the exposure time increased.
3. The large elemental γ/γ′ partitioning ratio of Re in 6.5 at. % Cr was the key factor that promoted the nucleation of the σ phase.

6. Acknowledgments

This work was supported Natural Science Foundation of China in grants (No. 91860202. No.51872008) and Beijing Natural Science Foundation (No.1182005, No. Z180014) and “111” project under the grand of DB18015.

7. References

[1] Mottura A, Reed RC. What is the role of rhenium in single crystal superalloys? *MATEC Web Conf* 2014 **14**
[2] Chen K, Zhao LR, Tse JS. Synergetic effect of Re and Ru on γ/γ′ interface strengthening of Ni-base single crystal superalloys. *Mater Sci Eng A* 2003 **360** 197–201
[3] Acharya M., Fuchs G. The effect of long-term thermal exposures on the microstructure and properties of CMSX-10 single crystal Ni-base superalloys. *Mater Sci Eng A* 2004 **381** 143–153
[4] Hobbs RA, Zhang L, Rae CMF, et al. TCP suppression in a ruthenium-bearing single-crystal nickel-based superalloy. *JOM* 2008 **60** 37–42

[5] Hobbs RA, Zhang L, Rae CMF, et al. Mechanisms of Topologically Close-Packed Phase Suppression in an Experimental Ruthenium-Bearing Single-Crystal Nickel-Base Superalloy at 1100 {\textdegree}C. *Metall Mater Trans A* 2008 **39** 1014–1025
[6] Ge BH, Luo YS, Li JR, et al. Distribution of rhenium in a single crystal nickel-based superalloy. *Scr Mater* 2010 **63** 969–972
[7] Cui CY, Osawa M, Sato A, et al. Effects of Ru additions on the microstructure and phase stability of Ni-base superalloy, UDIMET 720LI. *Metall Mater Trans A* 2006 **37** 355–360
[8] Rae CMF, Reed RC. The precipitation of topologically close-packed phases in rhenium-containing superalloys. *Acta Mater* 2001 **49** 4113–4125
[9] Smialek J, Meier GM. *High Temperature Oxidation in Superalloy*. 1987
[10] Reed RC. *The superalloys: fundamentals and applications*. Cambridge university press, 2008
[11] Pollock TM, Tin S. Nickel-Based Superalloys for Advanced Turbine Engines: Chemistry, Microstructure and Properties. *J Propuls Power* 2006 **22** 361–374
[12] Yang JX, Zheng Q, Sun XF, et al. Topologically close-packed phase precipitation in a nickel-base superalloy during thermal exposure. *Mater Sci Eng A* 2007 **465** 100–108
[13] Chen JY, Feng Q, Sun ZQ. Topologically close-packed phase promotion in a Ru-containing single crystal superalloy. *Scr Mater* 2010 **63** 795–798
[14] Horner IJ, Cornish LA, Witcomb MJ. A study of the Al Ni Ru ternary system below 50 at.% aluminium. *J Alloys Compd* 1997 **256** 213–220
[15] Feng Q, Nandy T., Pollock T. The Re (Ru)-rich δ-phase in Ru-containing superalloys. *Mater Sci Eng A* 2004 **373** 239–249
[16] Jingyang C, Bin Z, Qiang F, Lamei C and Zuqing S. Efects of Ru and Cr on γ/γ' microstructural evolution of Ni-based single crystal superalloys during heat treatment. *Acta Metall Sin* 2010 **46**(8) 897-906.
[17] Chen JY, Feng Q, Cao LM, et al. Improvement of stress–rupture property by Cr addition in Ni-based single crystal superalloys. *Mater Sci Eng A* 2011 **528** 3791–3798
[18] CHEN J, FENG Q, CAO L, et al. Influence of Ru addition on microstructure and stress-rupture property of Ni-based single crystal superalloys. *Prog Nat Sci Mater Int* 2010 **20** 61–69
[19] Sato A, Harada H, Yokokawa T, et al. The effects of ruthenium on the phase stability of fourth generation Ni-base single crystal superalloys. *Scr Mater* 2006 **54** 1679–1684
[20] Rae C, Karunaratne M, J Small C, et al. *Topologically Close Packed Phases in an Experimental Rhenium-Containing Single Crystal Superalloy*. 2000